

Article

Sap Flow Responses of the Endangered Species *Juniperus drupacea* Labill. to Environmental Variables in Parnon Mountain, Greece

Evangelia Korakaki * , Evangelia V. Avramidou , Alexandra D. Solomou , Stefanos Boutsios 
and Evangelia N. Daskalakou

Institute of Mediterranean and Forest Ecosystems, Hellenic Agricultural Organization—ELGO DIMITRA, Terma Alkmanos, Ilisia, P.O. Box 14180, 11528 Athens, Greece; eavramidou@elgo.gr (E.V.A.); asolomou@elgo.gr (A.D.S.); stboutsios@gmail.com (S.B.); edaskalakou@elgo.gr (E.N.D.)

* Correspondence: ekorakaki@elgo.gr; Tel.: +30-210-7782125 (ext. 141)

Abstract: In the face of ongoing climatic changes, understanding the species' sap flow responses is of crucial importance for adaptation and resilience of ecosystems. This study investigated diurnal variability and radial sap flux density (Js) in a natural *Juniperus drupacea* forest on Mt Parnon and determined the climatic factors affecting its total sap flow (Qs). Between July 2021 and March 2022, Granier-type sensors and automatic weather stations monitored Js of *J. drupacea* trees and environmental factors. Utilizing a multi-point sensor for Js radial profile variability, correction factors were applied to calculate (Qs), ranging from 4.78 to 16.18 L day⁻¹. In drier months of the study period (July–September), Qs progressively increased with increasing PAR and soil temperature, reaching a plateau at maximum values (app. 600 μmol m⁻² s⁻¹ and 26 °C respectively) indicating partial stomatal closure. Whereas, during the wetter period (October–March), when water was no longer a limiting factor, VPD and PAR emerged as significant controllers of stand transpiration. In this period, Qs responded positively to increasing soil water content (θ) only on days with high VPD (>0.5 kPa). The studied *J. drupacea* stand demonstrated adaptability to varying environmental conditions, crucial for the species' survival, considering anticipated climate change scenarios.

Keywords: sap flux; radial profile; sapwood depth; Syrian juniper; diurnal variation; Peloponnese



Citation: Korakaki, E.; Avramidou, E.V.; Solomou, A.D.; Boutsios, S.; Daskalakou, E.N. Sap Flow Responses of the Endangered Species *Juniperus drupacea* Labill. to Environmental Variables in Parnon Mountain, Greece. *Forests* **2024**, *15*, 431. <https://doi.org/10.3390/f15030431>

Academic Editors: Ning Du, Janusz Zwiazek and Wen-Qing Zhang

Received: 7 February 2024
Revised: 20 February 2024
Accepted: 21 February 2024
Published: 23 February 2024



Copyright: © 2024 by the authors. Licensee MDPI, Basel, Switzerland. This article is an open access article distributed under the terms and conditions of the Creative Commons Attribution (CC BY) license (<https://creativecommons.org/licenses/by/4.0/>).

1. Introduction

The Mediterranean region has been identified as both a climate change [1,2] and a biodiversity hotspot [3]. Consequently, even slight modifications in the climate can lead to alterations in the Mediterranean region's flora and fauna, affecting the expansion, composition, and functioning of the ecosystems. Therefore, it is crucial to investigate and monitor isolated and fragmented populations, such as *Juniperus drupacea* Labill. This species is geographically restricted to Southeast Turkey, Western Syria, Israel, and Lebanon [4] and in Southern Greece, which is the only European locality. In Greece, *J. drupacea* is restricted in the southeastern Peloponnese region, particularly in Mt Parnon, where the majority of the population is present, and in Mt Taygetos where small patches have been found in a limited area [5–7].

Although *J. drupacea* is globally classified as a species of Least Concern [8], it is categorized as Endangered in Europe [9]. In Greece, the population of *J. drupacea* has been designated as a priority habitat (code: 9560*, Annex I of Directive 92/43/EEC) and is included in the network of Natura 2000 protected areas (code: GR 2520006) [10]. In addition, part of the *J. drupacea* forest in Mt Parnon, covering an area of 74 hectares, has been officially declared a “Preserved Monument of Nature” (FEK 121D/1980) and designated as an “Absolute Nature Protection Area” (Joint Ministerial Decision No. 33999-FEK 353/6 September 2010).

The nearly 40-year protection regime, coupled with the gradual abandonment of agricultural areas, has had a positive impact on the expansion of the *J. drupacea* in Mt Parnon, particularly on former farmlands [11]. Conversely, Walas et al. [12] noted that the global habitat range of *J. drupacea* was considerably wider in the past and raised concerns about the species' survival in light of projected climate scenarios and potential climate changes. They speculated that under a climate scenario with a 1 °C temperature increase, the area providing suitable conditions for *J. drupacea* would experience a significant reduction. Whereas, in a climate scenario with a 2 °C temperature increase, no suitable conditions for the species would be found within its current geographic range, mainly due to decreased precipitation and increased temperatures.

Climate change is expected to have significant effects on water availability in the Mediterranean Basin, primarily due to an increase in the frequency, intensity, and duration of drought periods [13]. This will result in a scarcity of moisture and high evapotranspiration during the summer season, leading to severe water stress in most plant species and triggering various ecological changes, such as modifications in photosynthetic activity, shifts in distribution limits, intensified competition among species and within the same species. Southern Europe, in particular, is projected to experience arid and warm conditions, which will increase tree transpiration and overall water loss in forest ecosystems while reducing soil moisture availability [14].

Hence, there is an increasing urgency to study physiological parameters associated with water status and tree transpiration, as well as identify the climate factors that impact them. A frequently employed approach for assessing stand-level transpiration is the application of thermal methods of sap flow measurement [15]. This approach involves extrapolating predictions of the overall water usage of individual trees. These predictions rely on measurements obtained through thermal sap flux probes positioned within the conductive portion of the sapwood and then sap flux density (Js) measurements need to be upscaled to the tree level [16]. However, upscaling sap flux observations to whole-tree or stand levels, requires accounting for radial variability. Neglecting this could result in systematic errors in the total sap flow [17–23]. Such errors may lead to an overestimation [24–26] or underestimation [27–29] of total tree sap flow and water use. To overcome these uncertainties, efforts have been made to assess the radial variability in sap flux density among different trees [17,26,30–32], or correction factors have been developed to consider the spatial variation of sap flow with increasing sapwood depth [20,33–35]. Hence, acknowledging the radial variability is crucial when upscaling sap flux density measurements to precisely estimate the water balance at both the tree and stand levels. Tree sap flow is closely related to the abiotic environment. Various relationships between sap flow and meteorological and soil temperature and moisture factors have been reported in the literature, differing among regions and/or species [32,36–38]. Therefore, it is important to investigate the driving factors that control the different responses of tree species to climatic conditions.

Several studies have investigated the morphology and stand characteristics of *J. drupacea* [4,5,7,12], as well as its biology and ecology [39], and many have examined the water use in various *Juniperus* species [40–46]. However, none have specifically investigated the water use of *J. drupacea* and its ecophysiological responses to different climatic conditions. To the best of the authors' knowledge, only one paper addresses water relations of *J. drupacea*, but speculations are not based on field measurements but rather on observations [39]. In fact, in this paper authors noted that water relations should be confirmed in a field study. Another study has examined the relationship of *J. drupacea* of water potential with epigenetic and genetic diversity indexes and suggested that epigenetic diversity significantly influences the species' ability to withstand impending drought periods [47].

Understanding the water relations of *J. drupacea* and the environmental factors that impact them is essential for assessing the species' capacity to adapt and survive in arid and water-limited environments. The research presented in this paper is crucial for enhancing our understanding of the mechanisms employed by *J. drupacea* to adapt to changing climatic conditions. Thus, through the present study, we (a) assessed the diurnal variability of

sap flux density and the radial profile of a natural *J. drupacea* forest in Mt Parnon and (b) determined the climatic factors affecting its total sap flow, during the wetter and drier study period.

2. Materials and Methods

2.1. Description of Study Site

The study was conducted in a natural *J. drupacea* stand located in Mt Parnon, near Malevi Monastery, SE Peloponnese, Greece (latitude: 37°19' N, longitude: 22°35' E, altitude 950 m a.s.l.). The *J. drupacea* forest in Mt Parnon grows on limestone soils [48] and in this site, it forms a pure *J. drupacea* stand. In this stand, juniper trees appear as the dominant species, with a mean age of 25 years, mean tree height of 5.54 m, mean diameter at breast height of 10.55 cm, density of 400 individuals per hectare, and Leaf Area Index (LAI) of 3.601. Tree height measurements were performed with the stick method for trees with a height below 6 m and a Nikon 550 Forestry Pro II laser hypsometer (accuracy of ± 0.3 m, Nikon Vision, Tokyo, Japan) was used for taller trees. The diameter at breast height (1.3 m) (D) was measured with a caliper, and the LAI was estimated using an LAI-2200 Plant Canopy Analyzer (PCA) (LI-COR Inc., Lincoln, NE, USA). Four above-canopy observations were initially conducted as reference readings in a nearby opening to minimize variations in incoming radiation. Then, eight below-canopy measurements were taken along each of the three transects within the plot and the average LAI value was computed to represent the sample plot. The measurements were conducted in July 2021 during the early morning, prior to the onset of direct sunlight hours, under stable clear sky conditions.

The area has a relatively high level of humidity compared to the Mediterranean climate [49]. The mean air temperature is 13 °C, the mean annual rainfall is 1403 mm (ranging from 131 mm in summer to 517 in winter), and the average annual evapotranspiration (ET_o) is 1077 mm. Xerothermic season lasts about 1.5 months, from July to mid-August and the rainy season starts in October [50].

2.2. Environmental Variables

A fully automated and telemetric meteorological station was installed approximately 5 m away from the *J. drupacea* stand, in a forest opening, in early July 2021. Micrometeorological data were taken every 10 s and averaged every 10 min. The recorded parameters included air temperature (°C), air relative humidity (%), photosynthetically active radiation (PAR, $\mu\text{mol m}^{-2} \text{s}^{-1}$), global solar radiation (W/m^2), wind speed (m/s) and direction (°), precipitation (mm), soil water content (%) and temperature (°C) at 5, 8 and 15 cm depth. Vapor pressure deficit (VPD, kPa) was also calculated from relative humidity and air temperature data.

2.3. Sapwood Area Determination and Sapwood Area Allometric Equation

To determine sapwood area, 41 *J. drupacea* individuals were cored with an increment borer (Haglöf increment borer, Torsång, Sweden), ranging in D from 1 to 37 cm. The sapwood depth at breast height was measured using a caliper. Sapwood could be easily differentiated from the heartwood. Tree age was also derived from the same wood core samples. The height (m) and D (cm) of all sampled trees were measured.

A relationship between sapwood area and D was described by a power function that best fitted our data ($R^2 = 0.9656$, $p < 0.0001$, Figure S1):

$$A_s = 0.3893D^{2.1239}, \quad (1)$$

where A_s is sapwood area (cm^2) and D is the diameter at breast height (cm).

The abovementioned Equation (1) was applied to estimate the sapwood area of the trees used for sap flux measurements (Table 1), and also used to calculate sap flow per unit sapwood area ($Q_s; \text{L h}^{-1}$).

Table 1. Tree characteristics of the monitored *Juniperus drupacea* individuals.

Tree ID	Height (m)	D (cm)	As (cm ²)	Age (yrs)
Tree 1	6.4	11.6	70.3	27
Tree 2	5.8	11.8	73.6	29
Tree 3	4.2	9.90	50.7	29
Tree 4	8.4	19.4	211.6	33
Tree 5	5.3	15.1	123.4	31

2.4. Sap Flux Density, Sap Flux Radial Profile, and Total Tree Sap Flow

Xylem sap flux density was monitored at five (5) *J. drupacea* trees using the thermal dissipation method [51,52]. In early July 2021, 2-cm long Granier-type sensors were installed at breast height (1.3 m), in the outer sapwood of the north-facing side of the stem. The two probes' vertical separation was approximately 12.0 cm, where the upper probe was constantly heated with constant energy (200 mWatt DC), and the lower was unheated and recorded the wood's reference temperature. All stems were insulated with reflective foil to minimize natural temperature gradients. The temperature difference between the two probes was recorded at 15-min intervals with a remote telemetry data logger (A760, Adcon, Klosterneuburg, Austria). Temperature differences were converted to sap flux densities based on the equation derived empirically by Granier [51,52]. The daily maximum temperature difference was used as an estimate of the temperature difference under zero flow conditions. Such conditions were scanned for 101 days spanning from July to November 2021, in accordance with the methodology outlined by Oishi et al. [16]. The maximum temperature differences between the probes exhibited stability over consecutive hours when VPD was below 0.05 kPa.

Sap flux, along with micrometeorological data were collected from July 2021 until March 2022. The analysis was based on a total of 212 days of sap flow monitoring data, excluding days with missing values caused by power supply malfunctions. In April 2022, the radial patterns of sap flux were examined during a single-day campaign. A commercially multi-point heat field deformation (HFD) sensor (HFD100, ICT International Pty Ltd., Armidale, Australia) was installed in the largest of the five sampled trees, which had a diameter (D) of 19.4 cm. The sensor was inserted at breast height, on the same side as the Granier probes, but positioned at approximately 15 cm from them to avoid any potential interferences between the measuring systems. HFD probes were inserted at the four pre-defined distances and temperatures at eight different depths within the xylem (ranging from 0.5 cm to 7.5 cm) were recorded from 10 a.m. until 5 p.m. at one-minute intervals. The HFD-derived temperature differences were used to calculate radial sap flux density in the various sections ($J_{s,i}$; cm³ cm⁻² h⁻¹), using the Sap Flow Tool software (v1.4, ICT International Pty Ltd., Armidale, Australia). The Sap Flow Tool software calculates sap flux densities based on equations derived by Nadezhdina et al. [53] and Poyatos et al. [35]. The last four xylem depths (4.5, 5.5, 6.5, and 7.5) were not considered since the displayed negative values are an indication that the xylem was not conductive at these depths or there was a reverse flow [53].

The sap flow per conducting sapwood area (Q_s ; cm³ h⁻¹) for tree 4 was calculated as a weighted mean according to Poyatos et al. [35] as follows:

$$Q_s = J_{0.5}A_{s,0.5} + J_{1.5}A_{s,1.5} + J_{2.5}A_{s,2.5} + J_{3.5}A_{s,3.5} + J_{3.5}A_{s,in} \quad (2)$$

where $J_{s,i}$ is sap flux density at each measuring depth, $A_{s,i}$ is the corresponding annulus area and $A_{s,in}$ is the conducting area beyond the influence of the last measuring point (deeper than 3.5 cm).

Since HFD measurements in Tree 4 were conducted simultaneously with the heat dissipation 2-cm long Granier sensor, we were able to relate sap flux density ($J_{s,i}$) at the four measuring depths with sap flux densities of single-point measurements at the depth of 2 cm, and obtain radial correction factors, as described in Poyatos et al. [35]. The correction

factors were then applied to account for the specific sap flux density profile in each of the remaining four study trees. Subsequently, Q_s were calculated using Equation (2), to upscale measurements to the tree level. In this context, a slight modification was made to Equation (2) where the depth of 2.5 cm was considered as the final measuring point (along with $A_{s,in}$), accounting for the shallower conductive sapwood present in the remaining four trees. Daytime values of Q_s were summed to describe total sap flow ($L \text{ day}^{-1}$).

2.5. Data Analysis

Statistical analysis and data visualization were performed with Sigmaplot software (v15.0, Inpixon, Palo Alto, CA, USA). Relationships of Q_s with environmental variables were examined using linear and non-linear regression analyses and coefficients of determination (R^2) for $p < 0.05$.

Days with any missing values, due to malfunctions in the power supply, were excluded from the analysis. For the development of mean diurnal curves of sap flux density (J_s), sap flow rates (Q_s), and environmental parameters, 30-min data were averaged in accordance with the frequency of data logging of sap flux and micrometeorological parameters. Then data were averaged on a daily basis for each measuring period for each tree ($n = 5$).

3. Results

3.1. Micrometeorological Conditions during the Study Period

Meteorological variables and sap flow were monitored from early July 2021 to late March 2022. The mean daily variations of VPD, PAR, air temperature (T_{mean}), soil temperature (T_{soil}), soil water content (θ) at 15 cm depth, and cumulative precipitation are presented in Figure 1. Mean daytime values of air temperature were 14.3 °C, VPD 1.02 kPa, PAR 591.9 $\mu\text{mol m}^{-2} \text{ s}^{-1}$, soil temperature 13.5 °C, soil water content 48.1%, and the total rainfall was 627.6 mm (Figure 1).

On average, the drier period, spanning from early July to early late September 2021, exhibited higher average air and soil temperatures, lower soil water content, and only a limited amount of rainfall (28.0 mm) was observed (Table 2). As a result, VPD was higher during this period compared to the October 2021 to March 2022 period. In the latter period, there was a substantial decrease in mean air temperature, resulting in low VPD values (<1.21 kPa), and both precipitation and soil water content started to increase, indicating that water was no longer a limiting factor (Table 2, Figure 1).

Table 2. Means of: air temperature (T_{mean}), vapor pressure deficit (VPD), photosynthetically active radiation (PAR), soil temperature (T_{soil}), soil water content (θ) at 15 cm depth, and sum of rainfall at the forest stand during the dry (July–September 2021) and wet (October 2021–March 2022) study periods (\pm SD).

Period	T_{mean} (°C)	VPD (kPa)	Precipitation (mm)	PAR ($\mu\text{mol m}^{-2} \text{ s}^{-1}$)	T_{soil} (°C)	θ (%)
Dry (July–Sept)	22.7 (\pm 4.0)	1.7 (\pm 0.8)	28.0 (\pm 1.7)	491.0 (\pm 115.6)	24.7 (\pm 3.0)	39.8 (\pm 1.0)
Wet (Oct–March)	6.6 (\pm 4.8)	0.3 (\pm 0.2)	599.6 (\pm 6.5)	186.6 (\pm 102.5)	8.2 (\pm 4.2)	52.2 (\pm 5.4)

3.2. Radial Profile Patterns of J_s , Total Tree Sap Flow (Q_s) and Its Responses to Environmental Variables

Sap flux densities were found to be higher in the outer xylem compared to the inner xylem and the mean sap flux density (J_{mean}) occurred slightly deeper than 1.5 cm from the cambium (Figure 2). Maximum sap flux densities were observed at a depth of approximately 0.5 cm from the cambium, while values declined towards a depth of 3.5 cm (Figure 3). Maximum J_s were 27.29 $\text{cm}^3 \text{ cm}^{-2} \text{ h}^{-1}$ and 14.79 $\text{cm}^3 \text{ cm}^{-2} \text{ h}^{-1}$ at the measurement depths

of 5 and 15 mm beyond the cambium, respectively. The maximum J_s in the two innermost depths (25 and 35 mm) was $10.03 \text{ cm}^3 \text{ cm}^{-2} \text{ h}^{-1}$ and $6.14 \text{ cm}^3 \text{ cm}^{-2} \text{ h}^{-1}$, respectively.

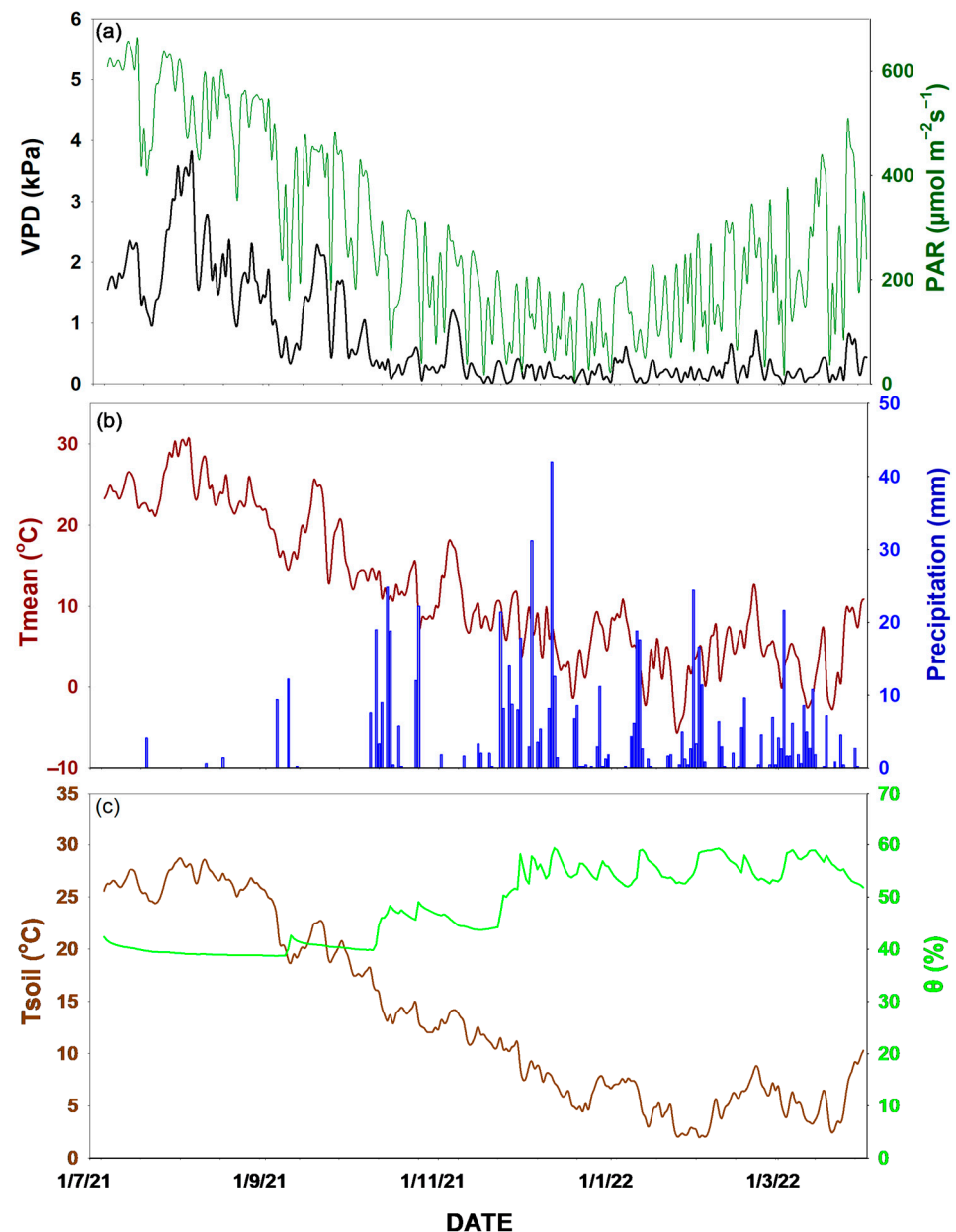


Figure 1. Daily values of: (a) vapor pressure deficit (VPD) and photosynthetically active radiation (PAR), (b) mean air temperature (T_{mean}) and precipitation, and (c) soil temperature (T_{soil}) and soil water content (θ) at 15 cm depth.

Mean monthly values of sap flow per conducting sapwood area ($Q_{S_{\text{mean}}}$) showed declining trends during the dry months of the study period (July to September 2021), corresponding to decreases in VPD and PAR. In November 2021, when water became available, $Q_{S_{\text{mean}}}$ increased (Figure 4) in line with the rising trend of soil water content (θ). From December 2021 until March 2022, when θ remained high (>47.2%), $Q_{S_{\text{mean}}}$ initially decreased until January 2022 and then increased towards February and March of the same years, following changes in VPD and PAR (Figure 1).

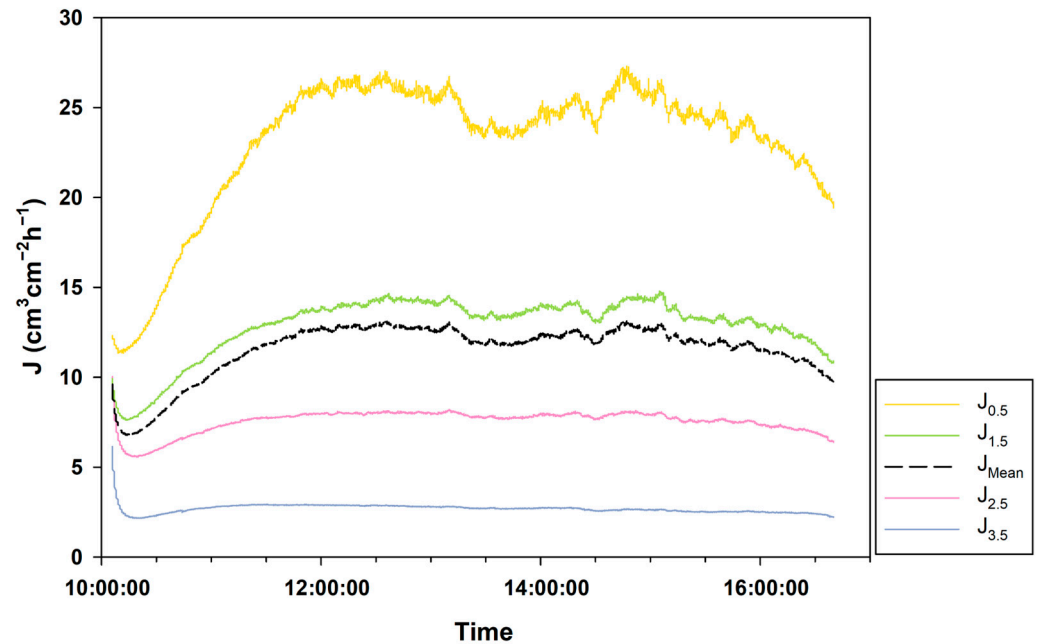


Figure 2. Radial sap flow densities $J_{s,i}$ [$\text{cm}^3 \text{cm}^{-2} \text{h}^{-1}$] were measured in a *Juniperus drupacea* tree at breast height using a multi-point HFD sensor inserted in different depths inside the sapwood. The outer depth was 0.5 cm and the inner was 3.5 cm of the functional sapwood.

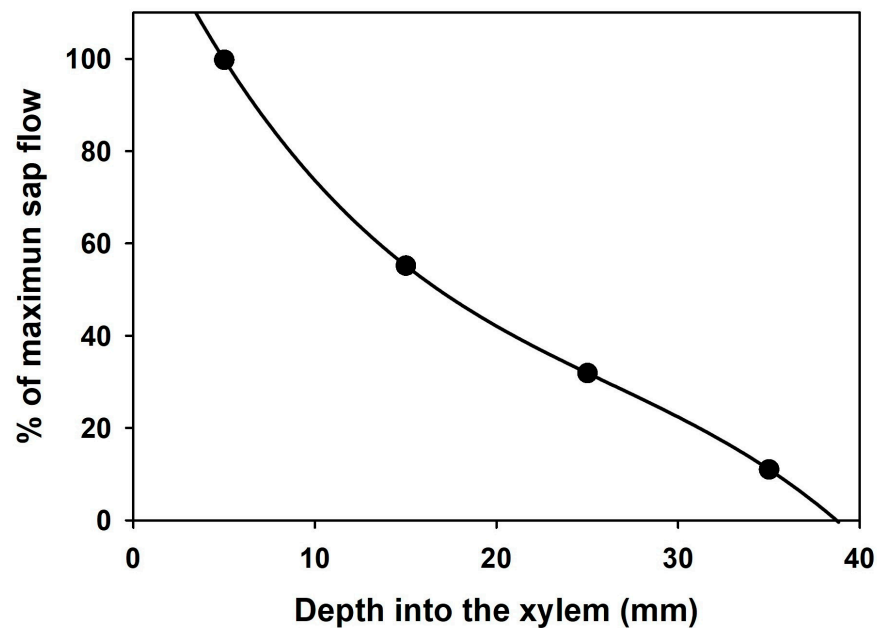


Figure 3. Sapwood depth estimation in a *Juniperus drupacea* tree from radial patterns of sap flow. Data points denote HFD measured values of sap flux density and the line is polynomial fit, used to extrapolate to the point of zero flow.

When total sap flow per conducting sapwood area (Q_s) values were regressed against VPD, PAR, T_{mean} , T_{soil} , and θ , during the drier period (July to early October 2021), it became evident that PAR ($R^2 = 0.5964$, $p < 0.001$, Figure 5a) and T_{soil} ($R^2 = 0.4205$, $p < 0.001$, Figure 5b) were the main controllers of Q_s . Q_s exhibited an increase with elevated PAR and T_{soil} , and a subsequent decline when T_{soil} reached a threshold of approximately 27°C ($R^2 = 0.7251$, $p < 0.0001$, Figure S2). Conversely, VPD, T_{mean} , and θ were not significantly related to Q_s , during the drier months of the study period.

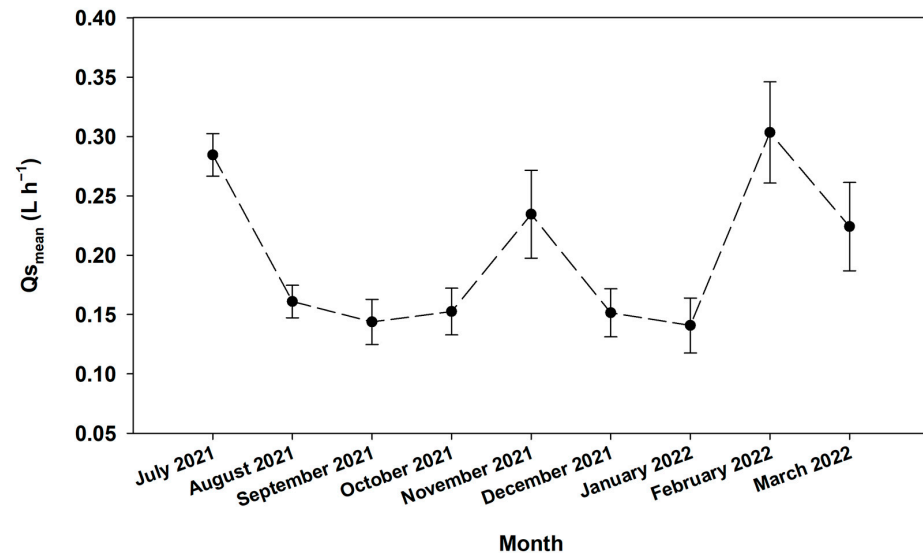


Figure 4. Mean monthly values of sap flow per conducting sapwood area $Q_{s_{\text{mean}}}$ [L h⁻¹] measured from July 2021 until March 2022. $n = 5$ trees \pm SE.

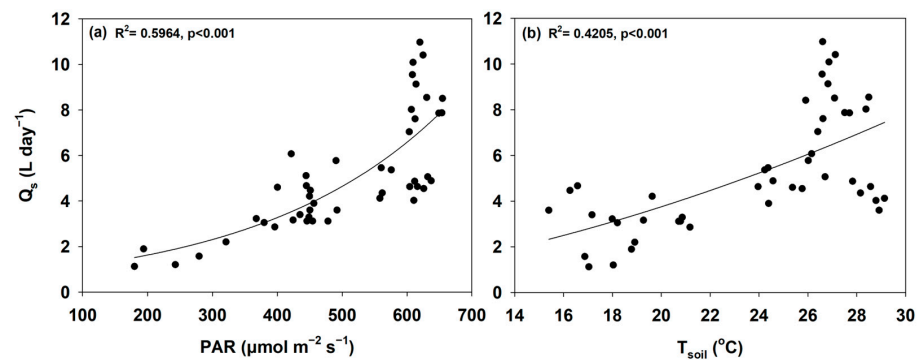


Figure 5. Relationships between Q_s [L day⁻¹] and (a) photosynthetically active radiation (PAR), and (b) mean soil temperature (T_{soil}) at 8 cm depth during the dry months of the study period (July to September 2021).

In the wetter period (October 2021 to March 2022), when water was no longer a limiting factor and soil water content (θ) exceeded 40%, VPD emerged as a strong and significant regulator of Q_s ($R^2 = 0.5501$, $p < 0.001$, Figure 6a). Additionally, PAR exhibited a less pronounced effect, yet still statistically significant ($R^2 = 0.2549$, $p < 0.001$, Figure 6b).

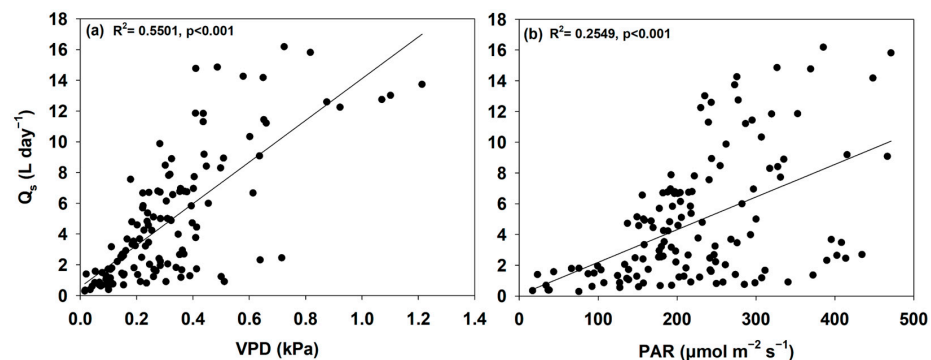


Figure 6. Relationships between Q_s [L day⁻¹] and (a) vapor pressure deficit (VPD), and (b) photosynthetically active radiation (PAR) during the wetter months of the study period (October 2021 to March 2022).

The impact of climate was additionally assessed across different VPD thresholds, revealing a significant influence of θ on Q_s during the wetter study period when VPD exceeded 0.5 kPa ($R^2 = 0.8303$, $p < 0.0001$, Figure 7). Nevertheless, it is essential to note that this correlation should be subjected to further investigation over an extended duration, as only 21 days experienced VPD levels exceeding 0.5 kPa.

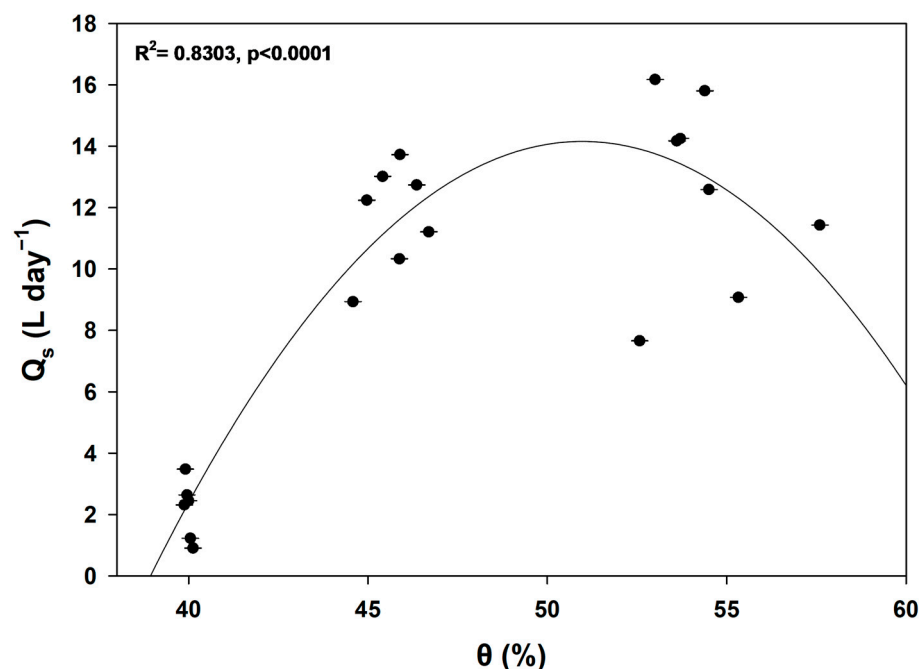


Figure 7. The relationship between Q_s [$L\ day^{-1}$] and soil water content (θ) during the wetter months of the study period (October 2021 to March 2022) is shown by the nonlinear regression model when VPD > 0.5 kPa). Symbols indicate mean daily values, and error bars indicate SE ($n = 5$ trees).

4. Discussion

In this study, we monitored the sap flow of *J. drupacea*, an endangered species with limited and fragmented distribution worldwide, in Mt Parion, located in the southeastern region of the Peloponnese, Greece. The aim was to investigate the species-specific water relations and identify the environmental variables that influence its water uptake and transpiration.

4.1. Sap Flow Radial Variability in *J. drupacea*

Sap flux density measurements were conducted at four different sapwood depths (0.5, 1.5, 2.5, and 3.5 cm) to account for the radial variability within *J. drupacea* trees when estimating total sap flow (Figure 2). Failing to account for this radial variability could introduce systematic errors when extrapolating sap flux density measured solely in the outer sapwood (typically at a 2 cm xylem depth) to estimate total sap flow and forest water use [17–23]. Such errors may result in either an overestimation of total tree sap flow and water use, especially in the case of conifers with deep functional sapwood [24–26], or conversely, an underestimation [27–29].

In our study, disregarding radial variability would have led to an underestimation of total sap flow by 57.1%. Similarly, Steppe et al. [28] reported a 60% underestimation of average sap flux density in *Fagus grandifolia* trees when employing the thermal dissipation method. Significant sap flow underestimations, reaching as high as 70%–95% in ring-porous species or in diffuse-porous and conifer species at very low sap flux densities, have also been documented [54]. A similar underestimation of tree transpiration, amounting to 37.5%, has been observed in Qinghai spruce [55]. On the contrary, other studies have indicated

overestimations of daily water use ranging from 27% to 90% in oak trees [23], 20.2% to 27.7% in Aleppo pine [26], and 5.6% in Qinghai spruce [32] when radial flux variability is neglected.

4.2. Total Tree Sap Flow Responses to Environmental Variables

Mean monthly values of sap flow per conducting sapwood area ($Q_{s,mean}$) varied throughout the study period, from 3.38 to 7.28 ($L\ day^{-1}$). Similar daily average water use values, ranging from 3.6 $L\ day^{-1}$ to 14 $L\ day^{-1}$, have been reported for Eastern Red cedar trees in Oklahoma, USA [45]. Another study documented monthly averaged transpiration rates of 2.95 $L\ d^{-1}$ in *Juniperus occidentalis* samplings in Oregon, USA, during August, when the precipitation exceeded its average value [56].

During the dry months (July to September) $Q_{s,mean}$ declined (Figure 4). These months are typically characterized by increased water stress, which could be attributed to the combination of high air temperature (max $T_{air} = 30.4\ ^\circ C$) and low soil moisture (min $\theta = 38.7\%$) (Figure 1). Interestingly, during this period, daytime total sap flow per conducting sapwood area (Q_s) displayed increasing trends in relation to photosynthetically active radiation (PAR) and soil temperature (Figure 5), but no significant correlation was observed with vapor pressure deficit (VPD), air temperature, or soil moisture.

In line with our results, previous studies have also reported a reduced sensitivity of physiological responses in various conifer species to VPD at low soil moisture levels [57,58]. For instance, Costa et al. [59] observed that VPD exerted control over sap flux in Aleppo pine only when a certain threshold of soil water availability was reached. Similarly, Korakaki and Fotelli [26] reported no significant effect of VPD on sap flow (Q_s) during two study periods when the soil water content was below 19%–20%. Furthermore, West et al. [40] suggested that the strong correlation they observed between sap flux and VPD in their study on transpiration controls in a *Pinus edulis* and *Juniperus osteosperma* woodland indicated that soil moisture was not a limiting factor.

In November 2021, when water became available (Figure 1), there was a corresponding increase in $Q_{s,mean}$ (Figure 4), aligning with the rising trend of soil water content (θ). During this wetter study period (October to March), marked by increased rainfall and soil water content (θ) exceeding 40%, VPD emerged as a significant controller of stand transpiration (Figure 6a). Additionally, Q_s displayed increasing trends in relation to PAR, but its effect was less pronounced (Figure 6b). Interestingly, no relationship between θ and Q_s could be established for the entire study duration. A significant impact of θ on Q_s was only detected during days of elevated evaporative demand when VPD exceeded 0.5 kPa (Figure 7). During these conditions, Q_s exhibited an increasing trend with elevated θ . When the θ surpassed 45%, Q_s appeared to stabilize at these favorable water moisture conditions (Figure 7). Upon reaching a high θ value (>45%), $Q_{s,mean}$ followed the changes in VPD and PAR. Consistent with our findings, studies in Aleppo pine in Greece [26] and Spain [59] showed that sap flow responded positively to increasing soil water levels on days with VPD higher than 0.7 and 0.5 kPa, respectively.

In soil moisture levels below 40%, sap flow in *J. drupacea* was primarily controlled by PAR and soil temperature, reaching a plateau at maximum values (approximately 600 $\mu mol\ m^{-2}\ s^{-1}$ and 26 $^\circ C$ respectively, Figure 4). This plateau occurred when VPD was high (>2.5 kPa), in July 2021, indicating a partial closure of stomata. Numerous studies have reported stomatal regulation in response to increasing VPD [60–62]. As VPD continues to rise, a plateau is reached, and eventually, sap flow declines at high VPD values [61,63,64], as observed in our results (Figure 2), suggesting stomatal closure. Stomatal closure in trees serves to reduce transpiration and prevent embolism in the xylem conduits of conifers [65]. When water availability increased, tree transpiration responded positively (Figures 1 and 4), likely due to a gradual refilling of previously cavitated tracheids [66].

According to Walas et al. [12], precipitation during the coldest three months (December to February) appeared to be the most influential factor in determining the current geographic range of *J. drupacea*. Precipitation contributed 41% to the entire range of the species and 47.5% to the populations in the Peloponnese. While temperature seasonality during the

wettest period had some influence on the species range prediction in Peloponnese (23.1%), it played a limited role in the worldwide distribution of *J. drupacea*.

The distribution and presence of *J. drupacea* in moderately thermophilic plant communities can be attributed to its light-demanding and drought-resistant characteristics [67,68]. Juniper species, including *J. drupacea*, possess physiological adaptations that allow them to efficiently extract water from deeper soil depths [43,69]. These characteristics played a crucial role in the survival of *J. drupacea* during the Pleistocene climate oscillations in mountainous regions. The species exhibited a migratory pattern, moving to lower elevations during cold glacial stages and to higher elevations during warm interglacial periods, which enabled its persistence in changing environments [12].

The studied *J. drupacea* stand displayed a remarkable adaptability to varying environmental conditions and showcased its capacity to respond to increased water availability from October to March. During this period, there was a positive response in sap flow to the favorable VPD and PAR conditions. Juniper species are capable of regulating stomatal transpiration for better water management during drought season [70] and have demonstrated tolerance to increasing summer drought with age [71].

The findings of this study highlight the potential of the endangered forest tree species, *J. drupacea*, to effectively overcome the adverse conditions during summer droughts and capitalize on more favorable water regimes occurring during autumn and winter. This ability is particularly critical for the survival and distribution of the remaining *J. drupacea* populations in SE Peloponnese, Greece, as they represent the sole population in Europe. Considering the projected future climate change scenarios, which anticipate rising air temperatures, elevated VPD, and changes in precipitation patterns in terms of frequency, intensity, and distribution [72], this adaptive capacity becomes even more essential for the species' long-term survival.

Additional research involving prolonged monitoring periods, such as collecting sap flow data over two consecutive years and encompassing tree activities throughout the growing season, could offer a more comprehensive understanding of how *J. drupacea* responds to environmental factors on a seasonal basis. This extended investigation would contribute to a deeper understanding of the species dynamics and provide valuable insights into its ecological responses and adaptations.

5. Conclusions

During the present study on *J. drupacea*, an endangered species with limited global distribution, we assessed the dynamics of sap flux densities and their radial variability in a natural stand in Mt Parnon, SE Peloponnese, Greece. Corrections were applied to sap flux densities and a power function was used to estimate sapwood area to upscale measurements to the tree level. We monitored the total sap flow ($Q_{S_{\text{mean}}}$) of *J. drupacea* and investigated the environmental factors influencing its transpiration. In the drier months of the study period, $Q_{S_{\text{mean}}}$ declined, while exhibiting a positive correlation with PAR and soil temperature, until a plateau was reached. During the wetter period, when soil water content was greater than 40%, $Q_{S_{\text{mean}}}$ increased with rising VPD, suggesting that VPD played a crucial role in regulating the transpiration of the studied *J. drupacea* stand. It seemed that *J. drupacea* demonstrated a drought-tolerant strategy in response to varying environmental conditions. These findings contribute to our knowledge of the water balance and adaptation strategies of *J. drupacea*, particularly in this the sole population in Europe, where information on the species' water relations is lacking.

Supplementary Materials: The following supporting information can be downloaded at: <https://www.mdpi.com/article/10.3390/f15030431/s1>. Figure S1: Non-linear relationship between the sapwood area and D developed from 41 sampled *Juniperus drupacea* individuals in Mt Parnon, SE Peloponnese, Greece ($p < 0.0001$). Figure S2: Q_s [$L \text{ day}^{-1}$] variation in relation to different mean soil temperatures (T_{soil}) at 8 cm depth during the dry months of the study period (July to September 2021). Non-linear regression line was generated using a Gaussian Peak Modified 5 parameter equation.

Author Contributions: Conceptualization, E.K.; methodology, E.K.; formal analysis, E.K.; data curation, E.K., E.V.A. and S.B.; writing—original draft preparation, E.K.; writing—review and editing, E.K., E.V.A., A.D.S., S.B. and E.N.D.; visualization, E.K.; project administration, E.N.D.; funding acquisition, E.N.D. All authors have read and agreed to the published version of the manuscript.

Funding: This research and the APC were funded by the European Regional Development Fund of the European Union and Greek national funds (2020–2022) through the Operational Program Competitiveness, Entrepreneurship and Innovation, under the call RESEARCH—CREATE—INNOVATE (project code: T2EDK-03378).

Data Availability Statement: The data presented in this study are available on request from the corresponding author.

Acknowledgments: The authors express their gratitude to the personnel of the Management Body of Parnon—Moustos—Mainalon & Monemvasia (N.E.C.C.A) for their valuable support in maintaining the operation of the meteorological station. The authors would also like to thank the Metropolitan of the Holy Metropolis of Mantinea and Kynouria, who allowed us to install the meteorological station on land owned by the Metropolitan. We especially thank the personnel of the General Directorate for Forests and Forest Environment of the Greek Ministry of Environment and Energy for granting us the research permit.

Conflicts of Interest: The authors declare no conflicts of interest.

References

- Giorgi, F. Climate change hot-spots. *Geophys. Res. Lett.* **2006**, *33*, 1–4. [\[CrossRef\]](#)
- Diffenbaugh, N.S.; Giorgi, F. Climate change hotspots in the CMIP5 global climate model ensemble. *Clim. Change* **2012**, *114*, 813–822. [\[CrossRef\]](#) [\[PubMed\]](#)
- Myers, N.; Mittermeier, R.A.; Mittermeier, C.G.; Da Fonseca, G.A.; Kent, J. Biodiversity hotspots for conservation priorities. *Nature* **2000**, *403*, 853–858. [\[CrossRef\]](#)
- Boratyfiski, A.; Browicz, K.; Zielifiski, J. *Chorology of Trees and Shrubs in Greece*; Institute of Dendrology, Polish Academy of Sciences: Kórnik, Poland, 1992.
- Tan, K.; Iatrou, G.; Johsen, B. *Endemic Plants of Greece: The Peloponnese*; Gads Forlag: Copenhagen, Denmark, 2001; Volume 1.
- Dimopoulos, P.; Raus, T.; Bergmeier, E.; Constantinidis, T.; Iatrou, G.; Kokkini, S.; Strid, A.; Tzanoudakis, D. *Vascular Plants of Greece: An Annotated Checklist—Englera 31*; Ser. Publ. Botanischer Garten und Botanisches Museum Berlin-Dahlem, Berlin and by Hellenic Botanical Society: Athens, Greece, 2013.
- Tan, K.; Sfikas, G.; Vold, G. *Juniperus drupacea (Cupressaceae) in the southern Peloponnese*. *Acta Bot. Fenn.* **1999**, *162*, 133–135.
- Gardner, M. *Juniperus drupacea*. In *The IUCN Red List of Threatened Species 2013: e. T30311A2792553*; International Union for Conservation of Nature and Natural Resources (IUCN): Gland, Switzerland, 2013.
- Rivers, M.; Beech, E.; Bazos, I.; Bogunić, F.; Buira, A.; Caković, D.; Carapeto, A.; Carta, A.; Cornier, B.; Fenu, G. *European Red List of Trees*; International Union for Conservation of Nature and Natural Resources (IUCN): Gland, Switzerland, 2019.
- Union, O.J.E.; Directive, H. Council Directive 92/43/EEC of 21 May 1992 on the Conservation of Natural Habitats and of Wild Fauna and Flora. *Off. J. Eur. Union* **1992**, *206*, 7–50.
- Daskalakou, E.; Oikonomidis, S.; Boutsios, S.; Ioannidis, K.; Thanos, C. Population characteristics of *Juniperus drupacea (Cupressaceae)* at the westernmost marginal area of its world distribution (Mt. Parnon, Greece). *Flora Mediterr.* **2022**, *32*, 305–316. [\[CrossRef\]](#)
- Walas, Ł.; Sobierajska, K.; Ok, T.; Dönmez, A.A.; Kanoğlu, S.S.; Dagher-Kharrat, M.B.; Douailhy, B.; Romo, A.; Stephan, J.; Jasińska, A.K. Past, present, and future geographic range of an oro-Mediterranean Tertiary relict: The *Juniperus drupacea* case study. *Reg. Environ. Change* **2019**, *19*, 1507–1520. [\[CrossRef\]](#)
- Spm-Ipcc-Wgii, I. *Summary for Policymakers*; Cambridge University Press: Cambridge, UK; New York, NY, USA, 2014.
- Bisselink, B.; Bernhard, J.; Gelati, E.; Adamovic, M.; Guenther, S.; Mentaschi, L.; De Roo, A. *Impact of a Changing Climate, Land Use, and Water Usage on Europe's Water Resources; A Model Simulation Study*; Joint Research Centre (JRC), Publications Office of the European Union: Luxembourg, 2018.
- Poyatos, R.; Granda, V.; Molowny-Horas, R.; Mencuccini, M.; Steppe, K.; Martínez-Vilalta, J. SAPFLUXNET: Towards a global database of sap flow measurements. *Tree Physiol.* **2016**, *36*, 1449–1455. [\[CrossRef\]](#)
- Oishi, A.C.; Oren, R.; Stoy, P.C. Estimating components of forest evapotranspiration: A footprint approach for scaling sap flux measurements. *Agric. For. Meteorol.* **2008**, *148*, 1719–1732. [\[CrossRef\]](#)
- Čermák, J.; Cenciala, E.; Kučera, J.; Hällgren, J.-E. Radial velocity profiles of water flow in trunks of Norway spruce and oak and the response of spruce to severing. *Tree Physiol.* **1992**, *10*, 367–380. [\[CrossRef\]](#)
- Cermak, J.; Nadezhdina, N. Sapwood as the scaling parameter-defining according to xylem water content or radial pattern of sap flow? In *Annales des Sciences Forestieres*; EDP Sciences: Les Ulis, France, 1998; pp. 509–521.

19. Lu, P.; Müller, W.J.; Chacko, E.K. Spatial variations in xylem sap flux density in the trunk of orchard-grown, mature mango trees under changing soil water conditions. *Tree Physiol.* **2000**, *20*, 683–692. [[CrossRef](#)] [[PubMed](#)]
20. Delzon, S.; Sartore, M.; Granier, A.; Loustau, D. Radial profiles of sap flow with increasing tree size in maritime pine. *Tree Physiol.* **2004**, *24*, 1285–1293. [[CrossRef](#)] [[PubMed](#)]
21. Fiora, A.; Cescatti, A. Diurnal and seasonal variability in the radial distribution of sap flux density: Implications for estimating stand transpiration. *Tree Physiol.* **2006**, *26*, 1217–1225. [[CrossRef](#)] [[PubMed](#)]
22. Reyes-Acosta, J.L.; Lubczynski, M.W. Optimization of dry-season sap flow measurements in an oak semi-arid open woodland in Spain. *Ecohydrology* **2014**, *7*, 258–277. [[CrossRef](#)]
23. Zhang, J.G.; He, Q.Y.; Shi, W.Y.; Otsuki, K.; Yamanaka, N.; Du, S. Radial variations in xylem sap flow and their effect on whole-tree water use estimates. *Hydrol. Process.* **2015**, *29*, 4993–5002. [[CrossRef](#)]
24. Berdanier, A.B.; Miniati, C.F.; Clark, J.S. Predictive models for radial sap flux variation in coniferous, diffuse-porous and ring-porous temperate trees. *Tree Physiol.* **2016**, *36*, 932–941. [[CrossRef](#)] [[PubMed](#)]
25. Si, J.; Feng, Q.; Yu, T.; Zhao, C. Nighttime sap flow and its driving forces for *Populus euphratica* in a desert riparian forest, Northwest China. *J. Arid Land* **2015**, *7*, 665–674. [[CrossRef](#)]
26. Korakaki, E.; Fotelli, M.N. Sap Flow in Aleppo Pine in Greece in Relation to Sapwood Radial Gradient, Temporal and Climatic Variability. *Forests* **2021**, *12*, 2. [[CrossRef](#)]
27. Hultine, K.; Nagler, P.; Morino, K.; Bush, S.; Burtch, K.; Dennison, P.; Glenn, E.; Ehleringer, J. Sap flux-scaled transpiration by tamarisk (*Tamarix* spp.) before, during and after episodic defoliation by the saltcedar leaf beetle (*Diorhabda carinulata*). *Agric. For. Meteorol.* **2010**, *150*, 1467–1475. [[CrossRef](#)]
28. Steppe, K.; De Pauw, D.J.; Doody, T.M.; Teskey, R.O. A comparison of sap flux density using thermal dissipation, heat pulse velocity and heat field deformation methods. *Agric. For. Meteorol.* **2010**, *150*, 1046–1056. [[CrossRef](#)]
29. Hölttä, T.; Linkosalo, T.; Riikonen, A.; Sevanto, S.; Nikinmaa, E. An analysis of Granier sap flow method, its sensitivity to heat storage and a new approach to improve its time dynamics. *Agric. For. Meteorol.* **2015**, *211*, 2–12. [[CrossRef](#)]
30. Nadezhdina, N.; Čermák, J.; Ceulemans, R. Radial patterns of sap flow in woody stems of dominant and understory species: Scaling errors associated with positioning of sensors. *Tree Physiol.* **2002**, *22*, 907–918. [[CrossRef](#)] [[PubMed](#)]
31. Ford, C.R.; McGuire, M.A.; Mitchell, R.J.; Teskey, R.O. Assessing variation in the radial profile of sap flux density in *Pinus* species and its effect on daily water use. *Tree Physiol.* **2004**, *24*, 241–249. [[CrossRef](#)] [[PubMed](#)]
32. Chang, X.; Zhao, W.; He, Z. Radial pattern of sap flow and response to microclimate and soil moisture in Qinghai spruce (*Picea crassifolia*) in the upper Heihe River Basin of arid northwestern China. *Agric. For. Meteorol.* **2014**, *187*, 14–21. [[CrossRef](#)]
33. Köstner, B.; Biron, P.; Siegwolf, R.; Granier, A. Estimates of water vapor flux and canopy conductance of Scots pine at the tree level utilizing different xylem sap flow methods. *Theor. Appl. Climatol.* **1996**, *53*, 105–113. [[CrossRef](#)]
34. Zang, D.; Beadle, C.; White, D. Variation of sapflow velocity in *Eucalyptus globulus* with position in sapwood and use of a correction coefficient. *Tree Physiol.* **1996**, *16*, 697–703. [[CrossRef](#)] [[PubMed](#)]
35. Poyatos, R.; Čermák, J.; Llorens, P. Variation in the radial patterns of sap flux density in pubescent oak (*Quercus pubescens*) and its implications for tree and stand transpiration measurements. *Tree Physiol.* **2007**, *27*, 537–548. [[CrossRef](#)]
36. Ma, C.; Luo, Y.; Shao, M.; Li, X.; Sun, L.; Jia, X. Environmental controls on sap flow in black locust forest in Loess Plateau, China. *Sci. Rep.* **2017**, *7*, 13160. [[CrossRef](#)]
37. Bosch, D.D.; Marshall, L.K.; Teskey, R. Forest transpiration from sap flux density measurements in a Southeastern Coastal Plain riparian buffer system. *Agric. For. Meteorol.* **2014**, *187*, 72–82. [[CrossRef](#)]
38. Zeng, X.; Xu, X.; Yi, R.; Zhong, F.; Zhang, Y. Sap flow and plant water sources for typical vegetation in a subtropical humid karst area of southwest China. *Hydrol. Process.* **2021**, *35*, e14090. [[CrossRef](#)]
39. Boratynski, A.; Donmez, A.; Bou Dagher-Kharrat, M.; Romo, A.; Tan, K.; Ok, T.; Iszkulo, G.; Sobierajska, K.; Marcysiak, K. Biology and ecology of *Juniperus drupacea* Labill. *Dendrobiology* **2023**, *90*, 1–29. [[CrossRef](#)]
40. West, A.; Hultine, K.; Sperry, J.; Bush, S.; Ehleringer, J. Transpiration and hydraulic strategies in a piñon–juniper woodland. *Ecol. Appl.* **2008**, *18*, 911–927. [[CrossRef](#)]
41. Mata-González, R.; Abdallah, M.A.; Ochoa, C.G. Water use by mature and sapling western juniper (*Juniperus occidentalis*) trees. *Rangel. Ecol. Manag.* **2021**, *74*, 110–113. [[CrossRef](#)]
42. Northup, A.P.; Keitt, T.H.; Farris, C.E. Cavitation-resistant junipers cease transpiration earlier than cavitation-vulnerable oaks under summer dry conditions. *Ecohydrology* **2022**, *15*, e2337. [[CrossRef](#)]
43. Mollnau, C.; Newton, M.; Stringham, T. Soil water dynamics and water use in a western juniper (*Juniperus occidentalis*) woodland. *J. Arid Environ.* **2014**, *102*, 117–126. [[CrossRef](#)]
44. West, A.; Hultine, K.; Burtch, K.; Ehleringer, J. Seasonal variations in moisture use in a piñon–juniper woodland. *Oecologia* **2007**, *153*, 787–798. [[CrossRef](#)]
45. Torquato, P.R. *Water Relation and Photosynthetic Performance of Eastern Redcedar (Juniperus virginiana) and Post Oak (Quercus stellata) in the Cross Timbers Forest*; Oklahoma State University: Stillwater, OK, USA, 2019.
46. Elhag, M.; Bahrawi, J. Evaluation of the transpiration character of *Juniperus macrocarpa* as an invasive species in western Crete, Greece. *Appl. Ecol. Environ. Res.* **2018**, *16*, 1659–1672. [[CrossRef](#)]
47. Avramidou, E.V.; Korakaki, E.; Malliarou, E.; Boutsios, S. Studying the Genetic and the Epigenetic Diversity of the Endangered Species *Juniperus drupacea* Labill. towards Safeguarding Its Conservation in Greece. *Forests* **2023**, *14*, 1271. [[CrossRef](#)]

48. Maerki, D.; Frankis, M. *Juniperus drupacea* in the Peloponnese (Greece). Trip report and range map, with notes on phenology, phylogeny, palaeontology, history, types and use. *Bull. CCP* **2015**, *3*, 3–31.
49. Cherlet, M.; Hutchinson, C.; Reynolds, J.; Hill, J.; Sommer, S.; Von Maltitz, G. *World Atlas of Desertification Rethinking Land Degradation and Sustainable Land Management*; Publication Office of the European Union: Luxembourg, 2018.
50. Proutsos, N.; Tigkas, D. Growth response of endemic black pine trees to meteorological variations and drought episodes in a Mediterranean region. *Atmosphere* **2020**, *11*, 554. [[CrossRef](#)]
51. Granier, A. A new method of sap flow measurement in tree stems. *Ann. For. Sci.* **1985**, *42*, 193–200. [[CrossRef](#)]
52. Granier, A. Evaluation of transpiration in a Douglas-fir stand by means of sap flow measurements. *Tree Physiol.* **1987**, *3*, 309–320. [[CrossRef](#)]
53. Nadezhdina, N.; Čermák, J.; Gašpárek, J.; Nadezhdin, V.; Prax, A. Vertical and horizontal water redistribution in Norway spruce (*Picea abies*) roots in the Moravian Upland. *Tree Physiol.* **2006**, *26*, 1277–1288. [[CrossRef](#)]
54. Xie, J.; Wan, X. The accuracy of the thermal dissipation technique for estimating sap flow is affected by the radial distribution of conduit diameter and density. *Acta Physiol. Plant.* **2018**, *40*, 88. [[CrossRef](#)]
55. Yang, J.; He, Z.; Lin, P.; Du, J.; Tian, Q.; Feng, J.; Liu, Y.; Guo, L.; Wang, G.; Yan, J. Variability in minimal-damage sap flow observations and whole-tree transpiration estimates in a coniferous forest. *Water* **2022**, *14*, 2551. [[CrossRef](#)]
56. Ochoa, C.G.; Abdallah, M.A. The Seasonal Variability and Environmental Factors Influencing the Transpiration of Western Juniper (*Juniperus occidentalis*) Saplings. *Hydrology* **2023**, *10*, 232. [[CrossRef](#)]
57. Alvarado-Barrientos, M.S.; Hernández-Santana, V.; Asbjornsen, H. Variability of the radial profile of sap velocity in *Pinus patula* from contrasting stands within the seasonal cloud forest zone of Veracruz, Mexico. *Agric. For. Meteorol.* **2013**, *168*, 108–119. [[CrossRef](#)]
58. Magh, R.-K.; Bonn, B.; Grote, R.; Burzlaff, T.; Pfautsch, S.; Rennenberg, H. Drought superimposes the positive effect of Silver Fir on water relations of European beech in mature forest stands. *Forests* **2019**, *10*, 897. [[CrossRef](#)]
59. Sánchez-Costa, E.; Poyatos, R.; Sabaté, S. Contrasting growth and water use strategies in four co-occurring Mediterranean tree species revealed by concurrent measurements of sap flow and stem diameter variations. *Agric. For. Meteorol.* **2015**, *207*, 24–37. [[CrossRef](#)]
60. Lange, O.L.; Lösch, R.; Schulze, E.-D.; Kappen, L. Responses of stomata to changes in humidity. *Planta* **1971**, *100*, 76–86. [[CrossRef](#)]
61. Monteith, J. A reinterpretation of stomatal responses to humidity. *Plant Cell Environ.* **1995**, *18*, 357–364. [[CrossRef](#)]
62. Oren, R.; Phillips, N.; Ewers, B.; Pataki, D.; Megonigal, J.P. Sap-flux-scaled transpiration responses to light, vapor pressure deficit, and leaf area reduction in a flooded *Taxodium distichum* forest. *Tree Physiol.* **1999**, *19*, 337–347. [[CrossRef](#)] [[PubMed](#)]
63. Jarvis, P.G. Stomatal response to water stress in conifers. In *Adaption of Plants to Water and High Temperature Stress*; Turner, N.C., Kramer, P.J., Eds.; John Wiley & Sons: New York, NY, USA, 1980; pp. 105–122.
64. Pataki, D.E.; Oren, R.; Smith, W.K. Sap flux of co-occurring species in a western subalpine forest during seasonal soil drought. *Ecology* **2000**, *81*, 2557–2566. [[CrossRef](#)]
65. Yoder, B.; Ryan, M.; Waring, R.; Schoettle, A.; Kaufmann, M. Evidence of reduced photosynthetic rates in old trees. *For. Sci.* **1994**, *40*, 513–527.
66. Tognetti, R.; Michelozzi, M.; Giovannelli, A. Geographical variation in water relations, hydraulic architecture and terpene composition of Aleppo pine seedlings from Italian provinces. *Tree Physiol.* **1997**, *17*, 241–250. [[CrossRef](#)] [[PubMed](#)]
67. Atalay, I.; Efe, R.; Öztürk, M. Ecology and classification of forests in Turkey. *Procedia-Soc. Behav. Sci.* **2014**, *120*, 788–805. [[CrossRef](#)]
68. Bergmeier, E. Plant communities and habitat differentiation in the Mediterranean coniferous woodlands of Mt. Parnon (Greece). *Folia Geobot.* **2002**, *37*, 309–331. [[CrossRef](#)]
69. Thurow, T.L.; Hester, J.W. How an increase or reduction in juniper cover alters rangeland hydrology. In *Juniper Symposium Proceedings*; Texas A&M University: San Angelo, TX, USA, 1997; pp. 9–22.
70. Abdallah, M.A.; Durfee, N.; Mata-Gonzalez, R.; Ochoa, C.G.; Noller, J.S. Water use and soil moisture relationships on western juniper trees at different growth stages. *Water* **2020**, *12*, 1596. [[CrossRef](#)]
71. Rozas, V.; DeSoto, L.; Olano, J.M. Sex-specific, age-dependent sensitivity of tree-ring growth to climate in the dioecious tree *Juniperus thurifera*. *New Phytol.* **2009**, *182*, 687–697. [[CrossRef](#)]
72. Stocker, T. *Climate Change 2013: The Physical Science Basis: Working Group I Contribution to the Fifth Assessment Report of the Intergovernmental Panel on Climate Change*; Cambridge University Press: Cambridge, UK, 2014.

Disclaimer/Publisher’s Note: The statements, opinions and data contained in all publications are solely those of the individual author(s) and contributor(s) and not of MDPI and/or the editor(s). MDPI and/or the editor(s) disclaim responsibility for any injury to people or property resulting from any ideas, methods, instructions or products referred to in the content.